Direct observation of nonlinear four-magnon scattering in spin-wave microconduits

H. Schultheiss,[1,2] K. Vogt,[2,3] and B. Hillebrands[2]

[1]*Materials Science Division, Argonne National Laboratory, 9700 S. Cass Avenue, Argonne, Illinois 60439, USA*

[2]*Fachbereich Physik and Forschungszentrum OPTIMAS, Technische Universität Kaiserslautern, D-67663 Kaiserslautern, Germany*

[3]*Graduate School of Excellence Materials Science in Mainz, Gottlieb-Daimler-Strasse 47, D-67663 Kaiserslautern, Germany*

(Received 7 June 2012; revised manuscript received 27 July 2012; published 10 August 2012)

We demonstrate the intrinsic nonlinear dynamics of spin waves due to four-magnon scattering processes in a micrometer sized permalloy stripe. Spin waves are excited by a microwave current transmitted through a coplanar waveguide and the spin-wave spectrum is locally probed by Brillouin light scattering microscopy for a wide range of excitation powers. We find a transition from a purely monochromatic excitation of spin waves at low microwave powers to a large broadening of the spectrum above a certain threshold power. The spectral distributions of the measured spin waves show a unique profile, which is in excellent agreement with theoretical expectations for four-magnon scattering processes.

DOI: 10.1103/PhysRevB.86.054414 PACS number(s): 75.30.Ds, 75.40.Gb, 75.78.−n

The transport of spin information is one of the great challenges in condensed matter physics and of fundamental importance for the further development of spintronic devices. Due to the high spin relaxation rate in metals, the information encoded in the spin polarization of electrons is lost within a few nanometers in the diffusive transport regime, making direct spin transport not very feasible. The recent discovery that a spin current can be transmitted over a macroscopic distance utilizing spin waves[1] has put great attention to the transport properties of spin waves. But there are obstacles that need to be overcome for utilizing spin waves as a carrier of information. In conventional ferromagnetic materials such as thin films of $Ni_{81}Fe_{19}$, for example, the spin-wave lifetime is of the order of a few nanoseconds and the group velocity, which accounts for the speed of information transport, does not exceed a few micrometers per nanosecond. Hence, spin-wave-driven information transport is limited to a few micrometers in case of inductive excitation.[2,3] This is still large compared to the spin diffusion length but there is a growing demand for new mechanisms for a more efficient excitation of spin waves, for example, via spin transfer torque,[4] or novel materials with a reduced magnetic damping.[5] The intrinsic nonlinear character of spin waves might pose a limitation to these approaches and might cause instabilities of the excited spin waves, which are known as Suhl instabilities or magnon-magnon scattering.[6] Both the excitation of higher amplitudes and a reduced damping will enhance these nonlinear effects. As a result, these processes can cause limitations of spin-wave currents.

Up to now, experimental evidence for these nonlinear mechanisms in metallic materials was only seen indirectly in time-resolved magneto-optical Kerr effect and ferromagnetic resonance measurements[7–9] and in the amplitude reduction of spin-wave pulses in the time domain.[10] Here, we report on the direct observation of these nonlinear mechanisms in the spin-wave spectrum and discuss them in terms of multimagnon processes in the description using second quantization, where a magnon is the quantum of excitation. In particular, we observe the process of four-magnon scattering, which is for most of the experimental geometries the lowest-order scattering process due to reasons discussed below. A consistent theoretical description of magnon-magnon scattering is tedious and was only developed for continuous thin films.[6,11] However, a basic understanding of the restrictions for magnon-magnon scattering can be derived from the energy and momentum conservation laws,

$$\sum_i^N \hbar\omega_i = \sum_j^M \hbar\omega_j \qquad \sum_i^N \hbar\vec{k}_i = \sum_j^M \hbar\vec{k}_j \tag{1}$$

The left (right) part of the equations summarizes over the initial (final) magnons with indices i (j) that are involved in the scattering process. The spin-wave frequencies $\omega_{i,j}$ and wave vectors $\vec{k}_{i,j}$ are connected via the spin-wave dispersion relation $\omega_{i,j}(\vec{k}_{i,j})$, which has a minimum frequency $\omega_0 = 2\pi\nu_0 \neq 0$ if a magnetic field[12,13] is applied. Below this frequency ω_0, no spin-wave eigenmodes exist, which immediately prohibits three-magnon scattering processes with $i = 1$ and $j = 2$ for $\omega_i < 2\omega_0$.[14] Similar considerations lead to the conclusion that four-magnon scattering processes with $i = 2$ and $j = 2$ are the lowest-order processes allowed in the frequency range $\omega_0 < \omega_i < 2\omega_0$ considering Eq. (1). In the presence of inhomogeneities wave-vector nonconserving two-magnon processes might appear in addition, which, however, can be suppressed by high sample quality.

The sample under investigation is a spin-wave microconduit consisting of a 2.5-μm wide and 100-μm long $Ni_{81}Fe_{19}$ stripe as shown in Fig. 1. The stripe has a thickness of 40 nm and was deposited in a ultrahigh vacuum chamber via molecular beam epitaxy. The patterning was made by means of electron beam lithography and chemical lift-off. One end of the spin-wave conduit is placed beneath the shorted end of a coplanar waveguide (CPW) with a thickness of 500 nm and a lateral width of 2 μm at the shorted end. A microwave current flowing in the CPW generates a dynamic Oersted field that excites spin waves inside the conduit. At the position of the shorted end of the CPW, the electric field is zero and, therefore, the microwave current reaches its maximum just above the spin-wave conduit. This allows for the excitation of spin waves with very high amplitudes driving the magnetic system into the strongly nonlinear regime. The spin-wave intensity is locally probed by a Brillouin light scattering (BLS) microscope,[15] which includes an active stabilization of the lateral sample position.

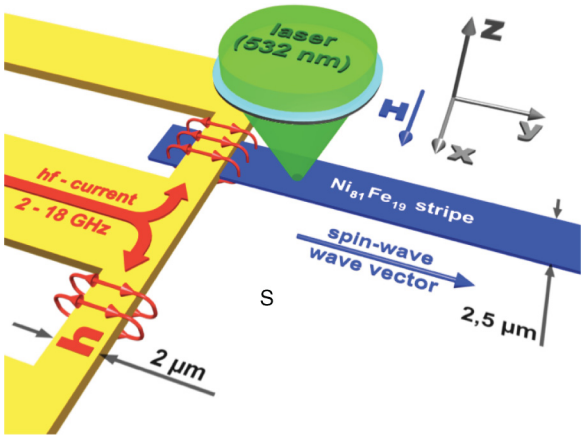

FIG. 1. (Color online) Schematic view of the sample. A 2.5-μm wide $Ni_{81}Fe_{19}$ microstripe acts as a spin-wave conduit and is placed under the shorted end of a coplanar waveguide. A microwave current creates a dynamic Oersted field **h** for exciting spin waves. The spin-wave intensity is locally probed by Brillouin light scattering (BLS) microscopy.

The spin-wave conduit was saturated by a magnetic field of 51 mT perpendicular to the conduit's long axis. In this geometry, the spin-wave dispersion relation for the first mode over the stripe width is monotonously increasing as shown by the solid red line in Fig. 2. The dispersion was calculated following the procedure given in Ref. 16 using standard material parameters for $Ni_{81}Fe_{19}$ as summarized in Ref. 17. The minimum frequency ν_0 for this specific geometry and magnetic field is 6.3 GHz. In the same figure we plot the normalized excitation efficiency of the 2-μm wide antenna (dashed blue line), given by the Fourier transformation of the excitation field distribution. The excitation efficiency has a local minimum at a wave vector of π μm^{-1}, which corresponds to a spin-wave frequency of 9.2 GHz. Within the frequency range 6.3GHz $< \nu_{RF} <$ 9.2GHz, spin waves can be excited by

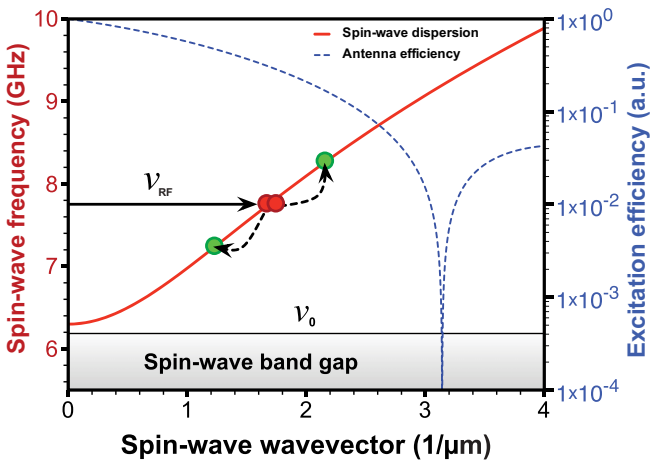

FIG. 2. (Color online) Spin-wave dispersion (solid red line) in the $Ni_{81}Fe_{19}$ microstripe with a magnetic field applied perpendicularly to the stripe's long axis. The dashed blue line shows the excitation efficiency of the antenna. The red and green circles illustrate a four-magnon scattering process when two spin waves, pumped at ν_{RF}, annihilate and create two new spin waves.

a RF current in the shorted CPW. As indicated by the red and green circles in Fig. 2, two of the directly excited magnons with frequency ν_{RF} can scatter and create two new magnons with frequencies $\nu_{RF} \pm \Delta\nu$ if the restriction $\Delta\nu < \nu_{RF} - \nu_0$ holds. Otherwise, one of the scattered magnons will have a frequency below ν_0. Except for the region close to $\vec{k} = 0$, the dispersion relation is approximately linear. Consequently, the momentum conservation holds for four-magnon scattering processes with $i = 2$ and $j = 2$ and $\omega_i = 2\pi\nu_{RF}$.

To observe the spin waves originating from these nonlinear processes experimentally, we locally measured the spin-wave spectra in 1-μm distance to the shorted end of the CPW as a function of the applied microwave frequency ν_{RF} for microwave powers ranging from 0 to 33 dBm. The experimental results are shown in Fig. 3 as intensity graphs. For each excitation frequency ν_{RF} (x axis), we acquired a spin-wave spectrum. The measured spin-wave frequencies are plotted on the y axis and the intensity is given by the color coded z axis.

For powers from 0 to 9 dBm, the response of the spin-wave conduit is the identity function. For higher powers, a significant broadening of the magnon spectra sets in. Apparently, the broadening of the spectrum does not cover the entire excitation frequency range for the intermediate power levels but is only visible up to a certain threshold excitation frequency marked with black arrows in the middle and lower row of Fig. 3. The reason for this cutoff frequency and the fact that for some graphs a vertical spike pattern is observed is a combination of the inherent nonlinear character of four-magnon scattering processes and the wave-vector-dependent excitation efficiency of the shorted CPW (see Fig. 2). The nonlinear scattering only takes place above a critical amplitude. But since we keep the output power of the microwave generator fixed when changing the excitation frequency, the intensity of the excited spin waves decreases with increasing ν_{RF} due to the reduced excitation efficiency of the CPW. The sharpness of this threshold frequency for which four-magnon scattering appears is directly related to the slope of the excitation efficiency. For smaller wave vectors (i.e., for smaller spin-wave frequencies) the excitation efficiency changes drastically as a function of the wave vector, whereas for higher frequencies the relative change in the excitation efficiency is much smaller (note the logarithmic scale of the right y axis in Fig. 2). As a consequence, the transition from line broadening to sharp resonance spectra is abrupt for a power of 18 dBm and gets smoother for increasing power values.

In the intensity graph for 18 dBm, we indicated the frequency boundaries for the scattered magnons. No magnon can be created below ν_0 and, hence, the upper frequency limit for four-magnon scattering is given by $2\nu_{RF} - \nu_0$ due to energy conservation. At frequencies close to ν_0, the dispersion is not linear so that momentum conversation suppresses four-magnon scattering.

The vertical spike pattern in the data close to the frequency threshold is a result of the frequency transmission characteristics of the CPW. Due to small impedance mismatches at the electrical contacts of the waveguide, the transmitted power varies as a function of ν_{RF}. If the system is close to the threshold power for four-magnon scattering, these small fluctuations become visible for varying ν_{RF}.

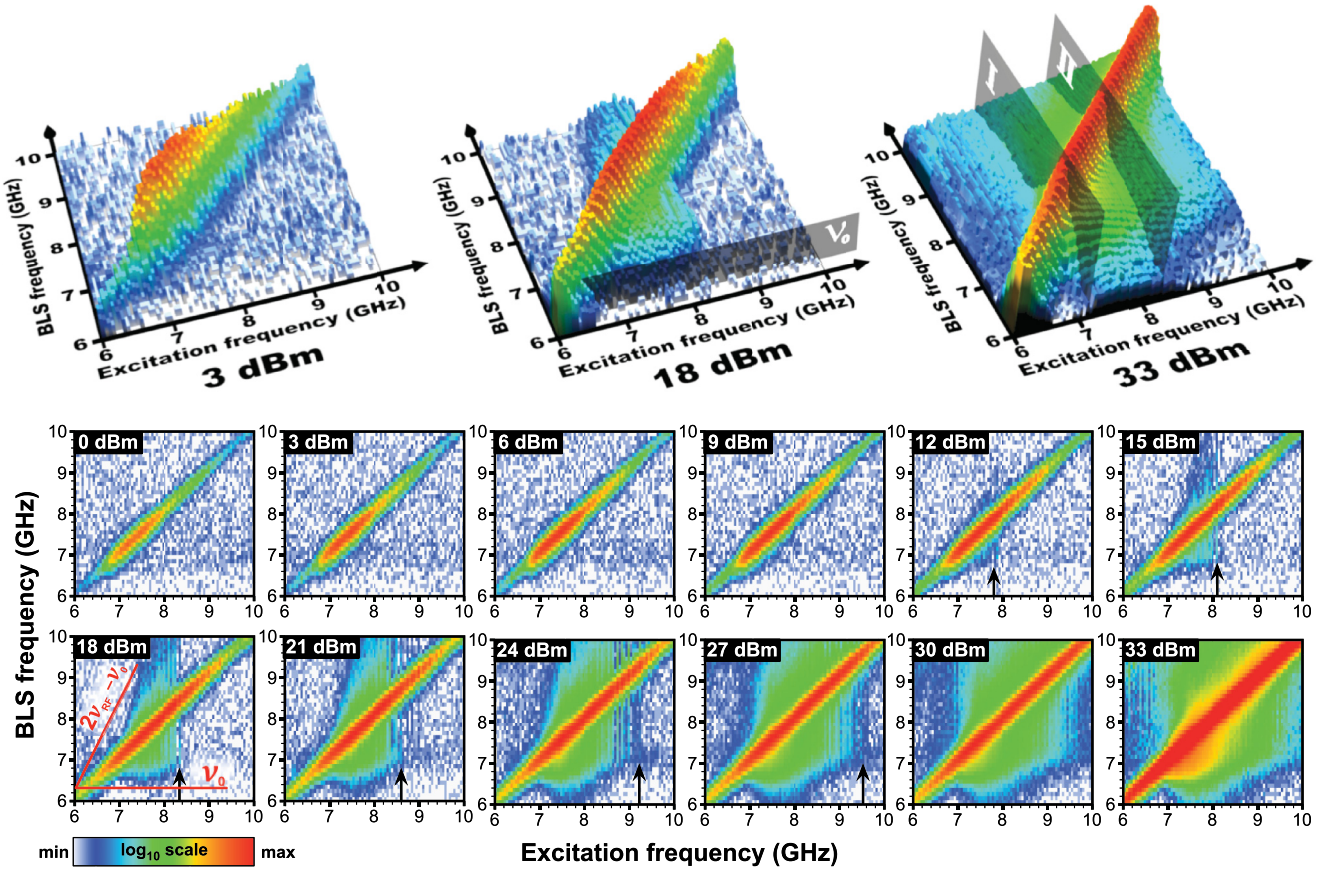

FIG. 3. (Color online) Top row: Spin-wave excitation spectra as a function of the applied microwave frequency ν_{RF} for three different power values: 3 dBm, 18 dBm, and 33 dBm. For each excitation frequency (abscissa) a spin-wave spectrum is locally measured close to the CPW by means of BLS microscopy. The spin-wave intensity (z axis) is color coded corresponding to the color scale shown at the bottom of the figure. In the middle graph the cutting plane depicts the minimum frequency of the spin-wave band. The planes (I) and (II) in the right graph display the frequencies for the power analysis of the spin-wave spectra in Fig. 4. Middle/bottom row: Two-dimensional (2D) projections of the spin-wave spectra as a function of the excitation frequency for various input powers. Arrows on the abscissa mark the frequencies up to which four-magnon scattering can be observed.

For a direct comparison of the spin-wave spectra as a function of the applied microwave power, we plotted the spectra normalized to the peak intensity for an excitation frequency of 7.1 GHz and 8.3 GHz in Fig. 4. These frequencies correspond to the planes (I) and (II) indicated in the upper right graph of Fig. 3. For both applied frequencies ν_{RF}, the broadening is clearly visible and one can see, that the main part of the scattered magnons is concentrated within the frequency interval $[\nu_0, 2\nu_{RF} - \nu_0]$. We want to point out that this line broadening cannot be described by a Lorentzian or Gaussian fit to the main resonance peak, which gives even more evidence that these are separate spin-wave eigenstates populated via four-magnon scattering.

For $\nu_{RF} = 7.1$GHz, an increase of the spin-wave intensities for frequencies even above $2\nu_{RF} - \nu_0$ is observed, which can be understood as repetitive scattering processes. Note, that the change in the linewidth (FWHM) of the directly excited spin waves caused by the additional damping due to four-magnon scattering cannot be resolved in our experiment, but the amplitude of the initial spin waves (red squares in Fig. 5 display the peak area of a Lorentzian fit) cannot be much further increased once the nonlinear scattering takes place.

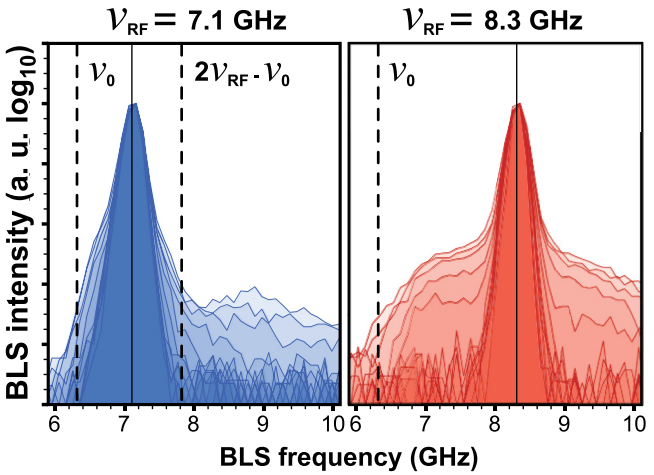

FIG. 4. (Color online) Spin-wave spectra for excitation at 7.1 GHz and 8.3 GHz corresponding to the planes (I) and (II) shown in Fig. 3. Different lines correspond to spectra at different applied microwave powers, normalized to the peak maximum.

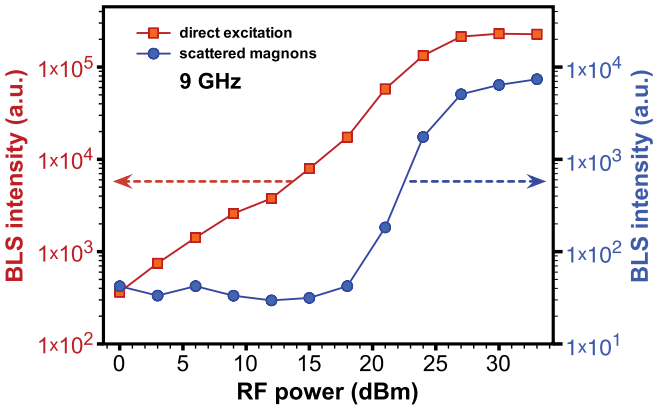

FIG. 5. (Color online) Intensity for the directly excited spin-wave at 9.0 GHz (red squares) and the integrated intensity of all spin waves generated by four-magnon scattering (blue circles).

At very high excitation powers, the intensity of the directly excited spin waves saturates because more and more energy is transferred to the scattered spin waves (blue circles in Fig. 5 display the total counts minus the peak area of the directly excited spin waves), which show a clear threshold as a function of the applied power.

In conclusion, we have demonstrated that the intrinsic nonlinear damping of spin waves via four-magnon scattering plays an important role for spin dynamics in small magnetic elements. The confinement of spin waves reduces the dimensionality of the dispersion relation compared to continuous thin films. Therefore, the scattered magnons have less eigenstates to populate, which leads to a faster growth of their amplitudes and, consequently, a faster onset of the nonlinear scattering. The direct observation of the scattered magnons in the BLS spectra allows for a deeper understanding of four-magnon scattering processes in microscopic magnetic elements and we believe that these results stimulate theoretical calculations of spin-wave instabilities in systems with reduced dimensionality. This is of crucial importance for future applications of spin waves in spintronic devices since these effects will be even more pronounced in novel magnetic materials with a reduced magnetic damping.

The authors thank P. Pirro and the Nano Structuring Center of the University of Kaiserslautern for their assistance in sample preparation and P. Krivosik, M. Wu, C.E. Patton, and A.A. Serga for fruitful discussions. Financial support by the German Research Foundation (DFG) is gratefully acknowledged. K.V. acknowledges financial support by the Carl Zeiss Foundation.

[1] Y. Kajiwara, K. Harii, S. Takahashi, J. Ohe, K. Uchida, M. Mizuguchi, H. Umezawa, H. Kawai, K. Ando, K. Takanashi, S. Maekawa, and E. Saitoh, Nature (London) **464**, 262 (2010).

[2] T. Sebastian, Y. Ohdaira, T. Kubota, P. Pirro, T. Brächer, K. Vogt, A. A. Serga, H. Naganuma, M. Oogane, Y. Ando, and B. Hillebrands, Appl. Phys. Lett. **100**, 112402 (2012).

[3] K. Sekiguchi, K. Yamada, S.-M. Seo, K.-J. Lee, D. Chiba, K. Kobayashi, and T. Ono, Phys. Rev. Lett. **108**, 017203 (2012).

[4] M. Madami, S. Bonetti, G. Consolo, S. Tacchi, G. Carlotti, G. Gubbiotti, F. B. Mancoff, M. A. Yar, J. Åkerman, Nature Nanotechnol. **6**, 635 (2011).

[5] T. Sebastian, Y. Ohdaira, T. Kubota, P. Pirro, T. Brächer, K. Vogt, A. A. Serga, H. Naganuma, M. Oogane, Y. Ando, and B. Hillebrands, Appl. Phys. Lett. **100**, 112402 (2012).

[6] H. Suhl, J. Phys. Chem. Solids **1**, 209 (1957).

[7] H. T. Nembach, K. L. Livesey, M. P. Kostylev, P. Martin-Pimentel, S. J. Hermsdoerfer, B. Leven, J. Fassbender, and B. Hillebrands, Phys. Rev. B **84**, 184413 (2011).

[8] T. Gerrits, P. Krivosik, M. L. Schneider, C. E. Patton, and T. J. Silva, Phys. Rev. Lett. **98**, 207602 (2007).

[9] H. M. Olson, P. Krivosik, K. Srinivasan, and C. E. Patton, J. Appl. Phys. **102**, 023904 (2007).

[10] V. E. Demidov, J. Jersch, K. Rott, P. Krzysteczko, G. Reiss, and S. O. Demokritov, Phys. Rev. Lett. **102**, 177207 (2009).

[11] A. Y. Dobin and R. H. Victora, Phys. Rev. Lett. **90**, 167203 (2003).

[12] C. Kittel, Phys. Rev. **110**, 1295 (1958).

[13] B. A. Kalinikos and A. N. Slavin, J. Phys. C **19**, 7013 (1986).

[14] H. Schultheiss, X. Janssens, M. van Kampen, F. Ciubotaru, S. J. Hermsdoerfer, B. Obry, A. Laraoui, A. A. Serga, L. Lagae, A. N. Slavin, B. Leven, and B. Hillebrands, Phys. Rev. Lett. **103**, 157202 (2009).

[15] H. Schultheiss, S. Schäfer, P. Candeloro, B. Leven, B. Hillebrands, and A. N. Slavin, Phys. Rev. Lett. **100**, 047204 (2008).

[16] K. Vogt, H. Schultheiss, S. J. Hermsdoerfer, P. Pirro, A. A. Serga, and B. Hillebrands, Appl. Phys. Lett. **95**, 182508 (2009).

[17] Saturation magnetization: $M_s = 880\,\mathrm{kA/m}$; gyromagnetic ratio: $\gamma = 28\,\mathrm{GHz/T}$; exchange constant: $A = 1.6 \times 10^{-11}\,\mathrm{J/m}$.